AIAA 81-0169R

Space Telescope Orbital Viewing Constraints

T.J. Sherrill*
Lockheed Missiles and Space Company, Inc., Sunnyvale, Calif.

Astronomical observations with the Space Telescope will be constrained by spacecraft operational requirements and capabilities, orbital viewing conditions, and the space environment. While ultraviolet or bright visual-range observations may be performed for 53-94.6 min per orbit (from a 500 km altitude), certain stray light sensitive experiments may be limited to 0-49 min of viewing per orbit. Careful operations scheduling may make possible observations of objects as close as 18 deg to the sun or of objects visible when the spacecraft is in a high-radiation environment. In all cases, mission planning beginning far in advance of actual observation performance will be required to make most efficient use of orbital viewing opportunities.

Introduction

THE Space Telescope (ST), illustrated in Fig. 1, is a nearly diffraction-limited 2.4 m telescope being developed under NASA control for Space Shuttle launch in early 1985, with a planned total mission life of 15 years. The Ritchey-Chrétien optical system will produce high-quality images over a large field of view. Five scientific instruments will share the inner portion of the telescope's focal plane, sampling light from the far ultraviolet to the near infrared; the initial instrument complement (replaceable at 2½ year intervals) consists of a wide-field and planetary camera, a faint object camera, a high-speed photometer, a high-resolution spectrograph, and a faint object spectrograph. Three fine guidance sensors will lock onto guide star pairs in the outer portion of the focal plane and in addition will provide capability for performing astrometric measurements. The expected performance of the ST scientific instruments has been detailed by Bahcall and O'Dell.[1]

Operating in a relatively low circular Earth orbit (nominally at 500 km altitude), the Space Telescope is subject to a wide variety of spacecraft and external environment constraints. Performance goals of observing objects of visual magnitude 27 or fainter and making exposures up to 10 h in length will place heavy demands on spacecraft stabilization systems and mission operations planning. It is a chief task in ST mission operations to determine how best to schedule experimental observations so as to make the most efficient use of available operational time within the framework of vehicle functions; viewing constraints due to the sun, Earth, moon, and other stray light sources; trapped particle radiation interference; onboard data storage capability; and communications opportunities.

Stray Light Viewing Constraints

Geometric Viewing Limits

The ST optical telescope assembly includes an internal light baffle system which will, in conjunction with an aperture door "sunshade," attenuate stray light from external sources. As illustrated schematically in Fig. 2, the goal is for the stray light illumination at the ST focal plane to be less than the equivalent diffused light from one 23rd (visual) magnitude star per square arc second when the telescope is viewing at an angle greater than 50 deg from the sun, 15 deg from the full moon, or 70 deg from the closest bright Earth point. This level was chosen to correspond approximately to the minimum level of zodiacal light near the ecliptic poles. The angles in the figure are design reference points rather than precise viewing restrictions; bright targets or targets observed in spectral regions for which sunlight is less of an interference can usually be scheduled closer to these bodies than indicated.

Even when the ST is in the terrestrial shadow or the closest Earth limb point is dark, there is generally an Earth angular limit closer than which an observation would not be scheduled because of atmospheric interference. For planning purposes a limit of 5 deg has usually been specified, corresponding to an atmospheric altitude of 200 km when the ST is at 500 km altitude. Figure 3 depicts the geometry of celestial viewing from a satellite orbit. Assuming that a target does not violate sun or moon constraints, it is clear from the figure that the unocculted viewing time depends primarily on the angular distance ζ of the object from the ST orbital plane. For a circular orbit and a limb angle constraint γ, the viewing time per orbit is given by the relation

$$t_v = \frac{T}{\pi}\cos^{-1}\left\{\frac{1}{\cos\zeta}\left[\frac{R_E}{R}\sin\gamma - \frac{\sqrt{R^2-R_E^2}}{R}\cos\gamma\right]\right\} \qquad (1)$$

where R_E is the Earth radius, R the orbit radius, and T the orbital period. Using a nominal altitude of 500 km and $\gamma = 5$ deg, this becomes

$$t_v = 0.5256\cos^{-1}\left(\frac{-0.2921}{\cos\zeta}\right)_{\text{deg}} \text{min} \qquad (2)$$

As seen from Fig. 3, the viewing time is a maximum, equal to the orbit period of 94.6 min, for $\zeta \geq 73.0$ deg, i.e., for target

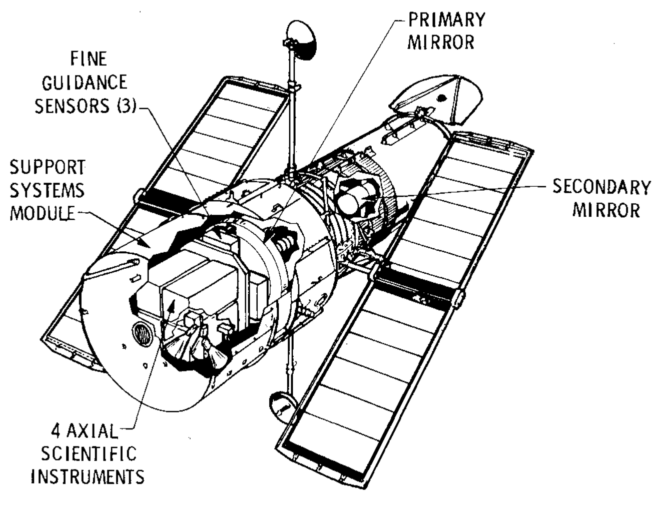

Fig. 1 Space Telescope.

Presented as Paper 81-0169 at the AIAA 19th Aerospace Sciences Meeting, St. Louis, Mo., Jan. 12-15, 1981; submitted Feb. 27, 1981; revision received July 13, 1981.

*Research Specialist, System Analysis Department, Space Systems Division. Member AIAA.

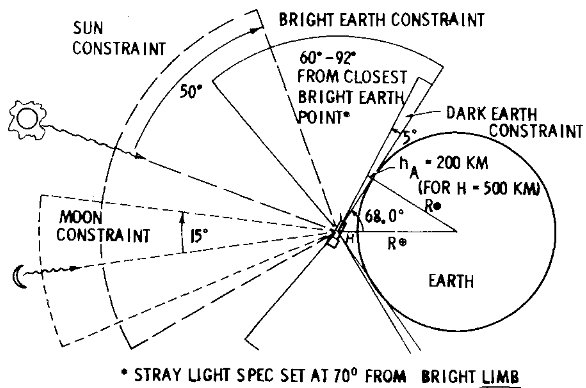

Fig. 2 Stray light constraint reference points for ST viewing.

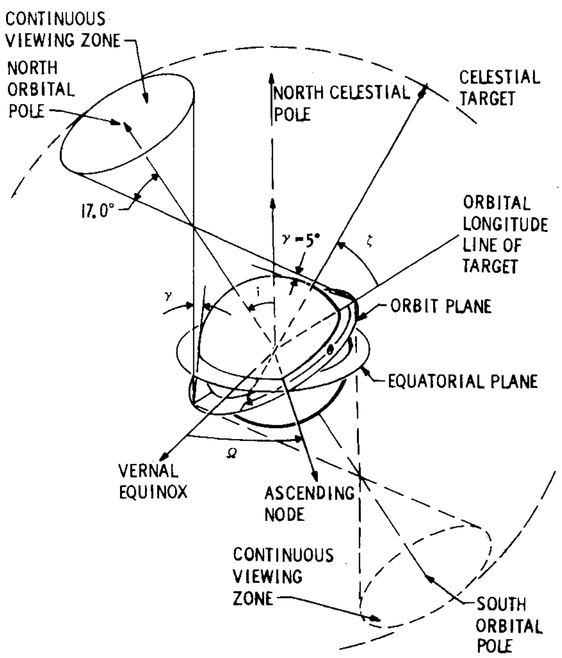

Fig. 3 Schematic of celestial viewing angles from a satellite orbit.

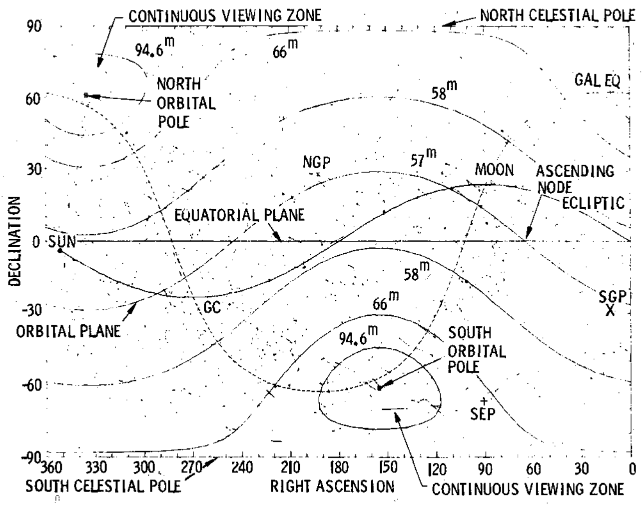

Fig. 4 Celestial viewing time contours for a representative 500 km orbit configuration ($\gamma = 5$ deg).

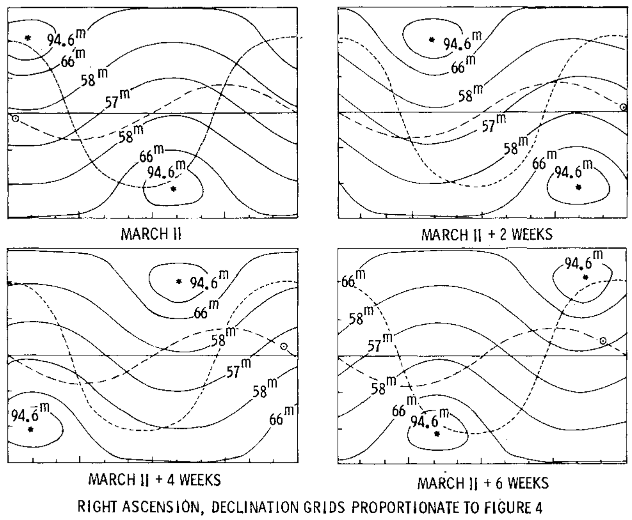

Fig. 5 Motion of celestial viewing contours over an ST nodal cycle (54 days) for a 500 km orbit ($\gamma = 5$ deg).

objects within 17.0 deg of the projected orbit poles; the two regions of the sky corresponding to this condition are called "continuous viewing zones." The minimum viewing time occurs for $\zeta = 0$, that is, for objects lying in the orbit plane, and is 56.2 min. It is obvious from Eq. (2) that for a given orbital orientation in space there will exist contours of equal visibility time on the celestial sphere, parallel to the "latitude" or "declination" lines of an orbital coordinate system. Figure 4 shows these contours for the nominal ST orbit, superposed on a map of the celestial sphere.[2] The contours are generated automatically using a mission operations computer program designated P/SOS (payload/spacecraft operations simulation).

For the Space Telescope orbital inclination $i = 28.5$ deg, the continuous viewing zones appear centered on the orbit poles at declinations 90 deg $- i = 61.5$ deg north and south of the equator, and at right ascensions 90 deg on either side of the right ascension of the orbital ascending node. If the Earth limb constraint angle were made more restrictive, e.g., if viewing were confined to objects more than $\gamma = 15$ deg from the Earth limb, the viewing times for all orbital latitudes ζ would be diminished. Likewise, the size of the continuous viewing regions would decrease.

Because the spacecraft orbital plane does not remain fixed in space but regresses (due to the Earth's oblateness) with respect to an equatorial inertial frame, the viewing time contours move in the direction of lower right ascensions (from left to right on the sky maps) in time. As shown in Fig. 5, the nominal ST orbit rotates through 360 deg in somewhat under 8 weeks (53.7 days), carrying the viewing contours with it.

Shadow Viewing Limits

An important consideration, especially for very faint targets, is the amount of time an object can be viewed while the ST is in the Earth's shadow. Although the telescope's light baffle system is intended to reduce the amount of stray light reaching the focal plane while the ST is in sunlight, many observations will still be restricted to viewing in the shadow plus a few minutes before and after. For a 500 km orbit at 28.5 deg inclination, shadow time ranges between 27.5 and 35.8 min (29.1-37.8% of the orbital period), depending upon the angle β between the Earth-sun line and the orbit plane. Figure 6 illustrates the variation of both β and shadow time over a year as the sun's declination changes and the ST orbital plane regresses in space. The extremes of the β variation occur near the solstices, when the sun is at its maximum/minimum declination of $\pm\epsilon$ (ϵ the obliquity of the ecliptic) and β can take on the values $\pm(i+\epsilon)$ or $\pm$ 51.9 deg.

From Fig. 7, it is clear that a celestial target is visible for the entire length of time that the spacecraft is in the Earth's shadow if its "orbital longitude" λ from the midshadow point obeys the relation

$$\lambda \leq \theta - \phi \tag{3}$$

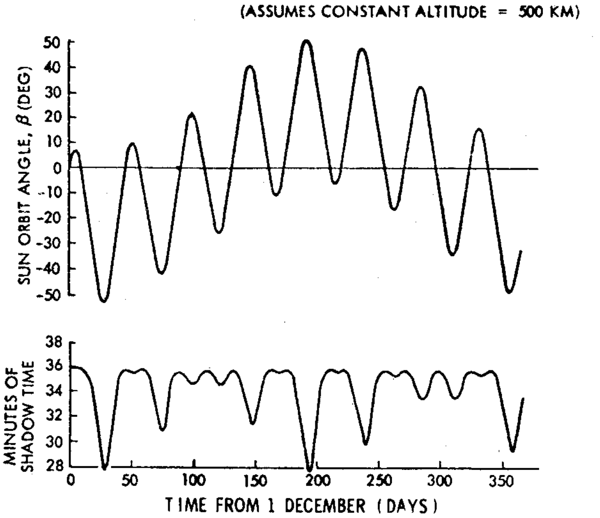

Fig. 6 Variation of sun-orbit beta angle and shadow time over one year.

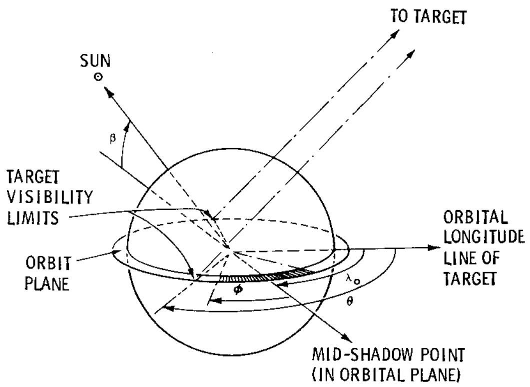

Fig. 7 Schematic of celestial viewing while in the Earth's shadow.

where θ is the half-angle of orbital longitude over which the object is visible,

$$\theta = \cos^{-1}\left\{\frac{1}{\cos\zeta}\left[\frac{R_E}{R}\sin\gamma - \frac{\sqrt{R^2 - R_E^2}}{R}\cos\gamma\right]\right\} \tag{4}$$

[cf. Eq. (1)] and ϕ is the half-shadow angle defined by

$$\phi = \cos^{-1}\left(\frac{\sqrt{R^2 - R_E^2}}{R\cos\beta}\right) \tag{5}$$

For a 500 km orbit and $\gamma = 5$ deg, Eq. (3) becomes numerically

$$\lambda \leq \cos^{-1}\left(\frac{-0.2921}{\cos\zeta}\right) - \cos^{-1}\left(\frac{0.3743}{\cos\beta}\right) \tag{6}$$

This equation can be thought of as defining a region of the celestial sphere in which objects are visible for 100% of the available shadow time. Figure 8 is a schematic representation of the "100% shadow viewing area" for a given time of the year; the two continuous viewing zones are always contained in this area. As the satellite orbit plane regresses in space, the orbit poles rotate around the celestial poles; hence the 100% shadow time region encompasses first the north, then the south, then the north celestial pole again, in the space of eight weeks. Near the orbital plane, the midshadow point and boundaries move more or less with the sun's rate, i.e., about 53 deg during the orbital regression period.

It can be shown that the condition [corresponding to Eq. (3)] for an object to be visible for at least 75% of the time that the spacecraft is in the Earth's shadow is given by the expression

$$\lambda < \theta - \tfrac{1}{2}\phi \tag{7}$$

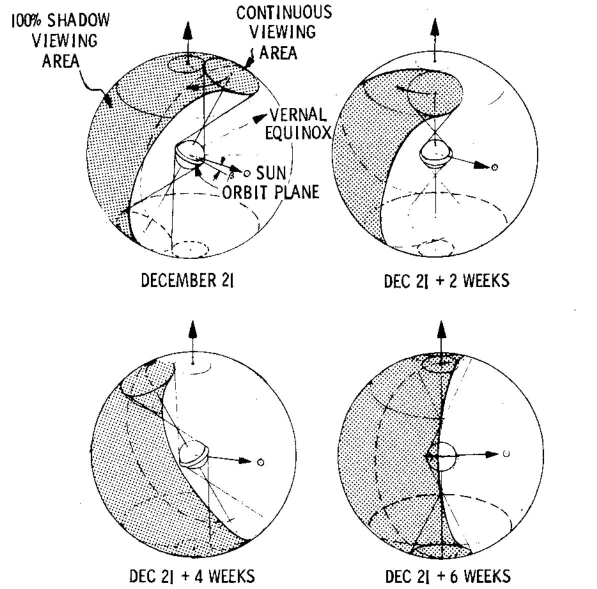

Fig. 8 Motion of the 100% shadow viewing area on the celestial sphere during ST nodal cycle.

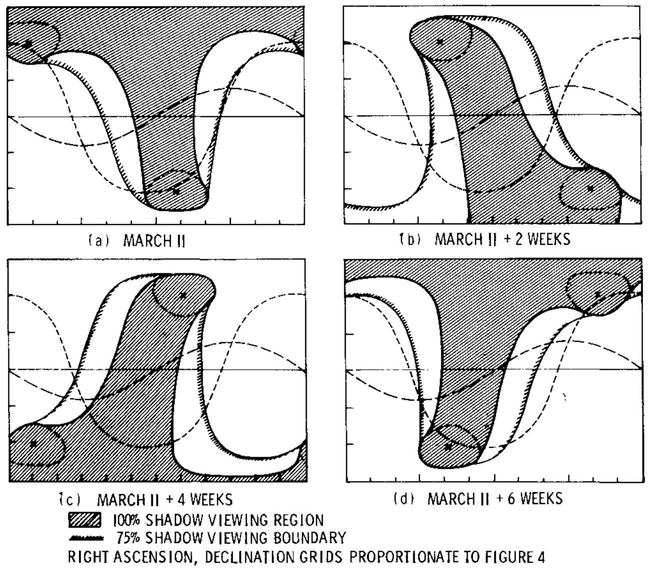

Fig. 9 Evolution of Earth occultation and shadow viewing constraints over an ST nodal cycle (54 days) for a 500 km orbit ($\gamma = 5$ deg).

Figure 9a shows the 100 and 75% shadow viewing areas plotted on a right ascension-declination sky grid. The boundaries of the former, for example, are plotted as the loci of points which satisfy the equality in Eq. (3).

Figures 9b-d show the evolution of the shadow viewing constraints over most of an orbit nodal cycle. Objects located near the celestial poles are seen to fall into either the continuous visibility zone or adjacent parts of the 100% shadow viewing area about every eight weeks, remaining there anywhere from a few days to four weeks or longer. On the other hand, objects which lie near the celestial equator, because of their proximity to the spacecraft orbital plane, fall into the central part of the 100% shadow viewing area once per year and remain there for a length of time which depends upon the "width" of this area for the particular time of year and orbital orientation involved. This width is given by

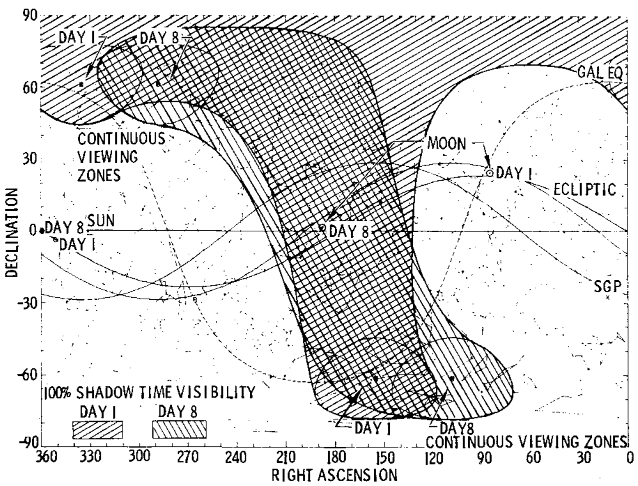

Fig. 10 Celestial shadow viewing regions over a one-week period (March 11-18).

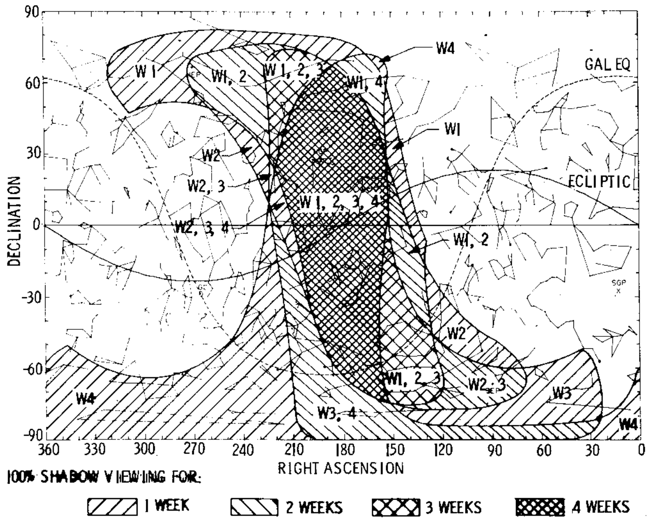

Fig. 11 100% shadow viewing opportunities over a four-week period beginning in mid-March.

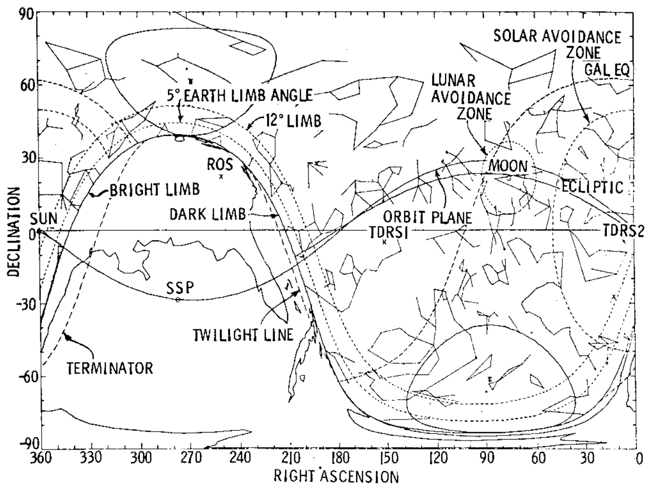

Fig. 12 "Snapshot" of Earth sunlit/shadowed regions from ST orbit.

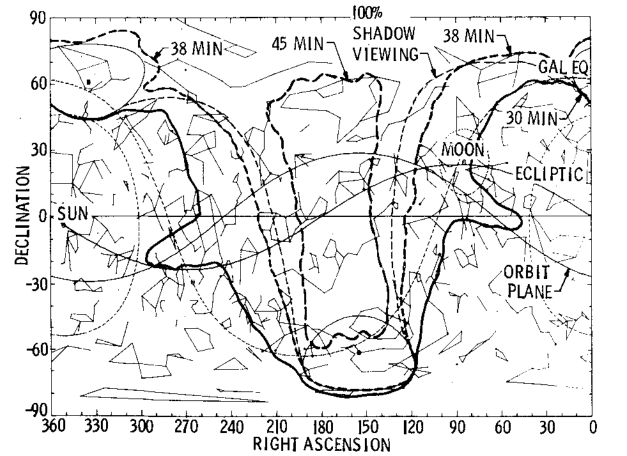

Fig. 13 Stray light constrained viewing time per orbit for 27th magnitude targets.

$2(\theta-\phi)$ [cf. Eq. (3)], and corresponds to 79-111 days of continuous shadow viewing. Thus, advance planning—perhaps a year ahead for many faint objects of interest—would be required to make the most efficient use of prime viewing time, and such planning could lead to very different viewing programs for objects at different locations in the sky.

If the 100% shadow viewing curves for two dates spaced seven days apart are superposed as in Fig. 10, then the area of overlap encompasses all targets visible throughout the Earth shadow during that week. If this idea is extended to a four-week period, Fig. 11 results. Although there is not a strict dichotomy between "sunlight targets" and "shadow targets" for ST observations, the figure is helpful in showing quite generally the regions of the sky which can be utilized most efficiently if a series of rather faint targets was to be scheduled during the four weeks. For example, targets in or near the regions denoted "W1" or "WI, 2" are best scheduled during the first two weeks of this time period, while those in or near the "W4" or "W3, 4" regions are best scheduled later.

Stray Light Constrained Viewing Limits

In actual practice astronomical observations will not be confined solely to Earth shadow periods; likewise, no single Earth limb angle constraint γ will apply to all Earth brightness conditions, that is, to viewing while in the Earth's shadow, while over a fully sunlit Earth, or when the sunlight terminator is being crossed. For example, as depicted in the orbital "snapshot" of Fig. 12, the western Earth limb might be bright and the eastern limb dark, with some residual atmospheric brightness in the region between the terminator and the "civil twilight line." NASA Marshall Space Flight Center utilizes a computer program entitled PSLIC (pseudo-stray light isochronal contours)[3] which models target pointing anywhere on the celestial sphere while integrating around a spacecraft orbit, establishing viewing cutoffs when the target is within 60-92 deg of the closest bright Earth point (the exact cutoff depending on object magnitude). Typical viewing time contours for 27th visual magnitude targets are displayed in Fig. 13. A maximum orbital viewing time of about 49 min, centered on the antisolar direction, is generally found for such very faint targets.

Figure 14 presents a comparison of PSLIC-generated stray light constrained viewing times with geometric Earth limb cutoff (5 deg dark/12 deg bright) viewing times, for observations of 20 representative objects suitable for viewing in the time frame depicted in Figs. 4 and 13 (mid-March). The proposed observations were in more than one spectral region for several of the targets, so that viewing time varies slightly with object magnitude in each region. Shadow and sunlight viewing portions for a typical orbit revolution are designated in the figure.

It is expected that in actual Space Telescope science planning some observations will be scheduled to tight Earth-reflected stray light constraints while others will be able to

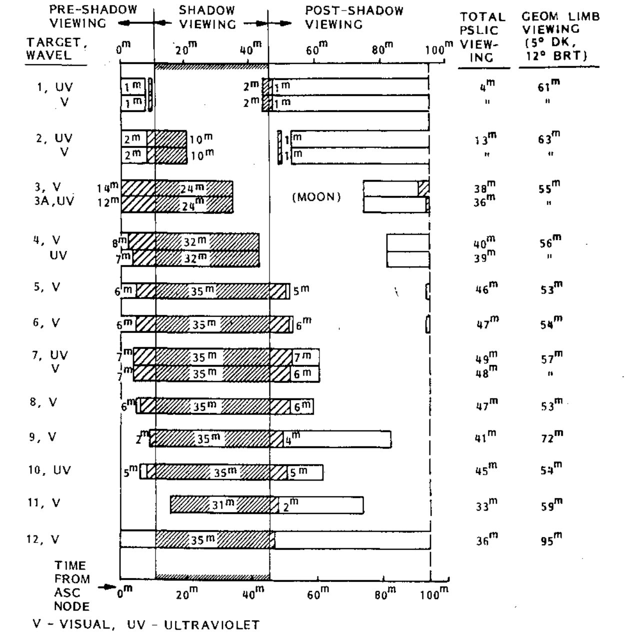

Fig. 14 Comparison of stray light sensitive and stray light insensitive viewing time per orbit for typical ST targets.

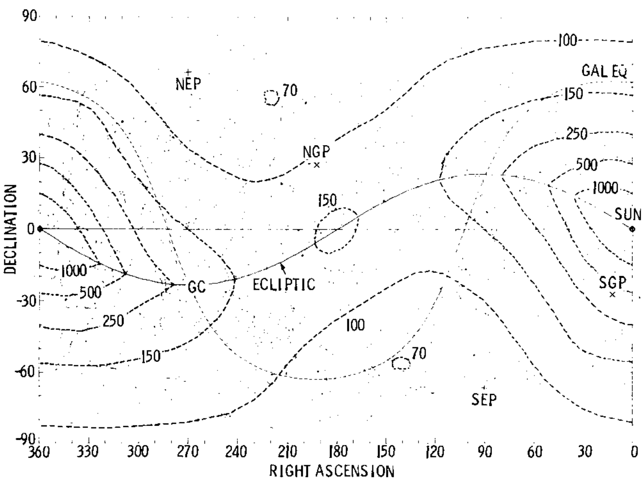

Fig. 15 Motion of zodiacal light S_{10} radiance contours over one year.

utilize less restrictive geometric viewing limits. An example of the less sensitive category of observations would be any experiment using an ST scientific instrument filter or grating at a wavelength shortward of about 2500 Å.

Zodiacal Light Constraints

Astronomical observations near the plane of the ecliptic will also be affected by sunlight reflected from dust or other particles concentrated in the fundamental plane of the solar system. While the interference discussed in earlier sections represents stray light from discrete sources which is reflected or scattered into the Space Telescope, this so-called zodiacal light is really a directly imaged "foreground" light source whose brightness is generally expressed in terms of S_{10} radiance levels, or the number of 10th (visual) magnitude stars per square degree required to produce an equivalent amount of radiation. Figure 15 depicts radiance contours due to Dumont[4] in the same (March) time frame as Figs. 4 and 9-14.The highest isophote delineated is $S_{10} = 1000$, extending ± 14 deg in latitude and ± 38 deg in longitude from the sun; the lowest contours, $S_{10} = 70$, lie 25 deg off the ecliptic poles. The $S_{10} = 150$ contour opposite the sun roughly defines the "gegenschein" or counterglow.

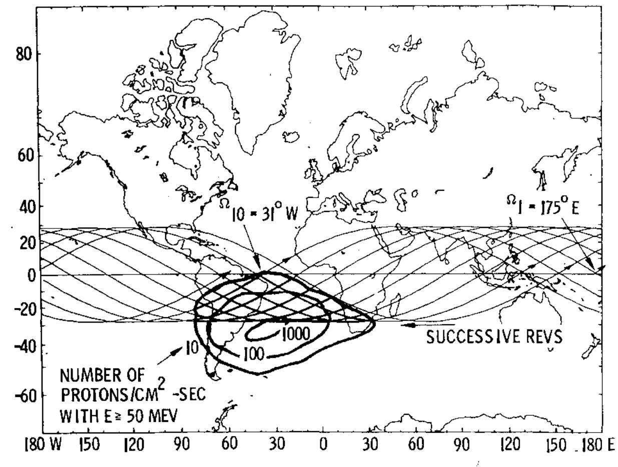

Fig. 16 Location of South Atlantic Anomaly contours relative to ST orbit at 500 km altitude.

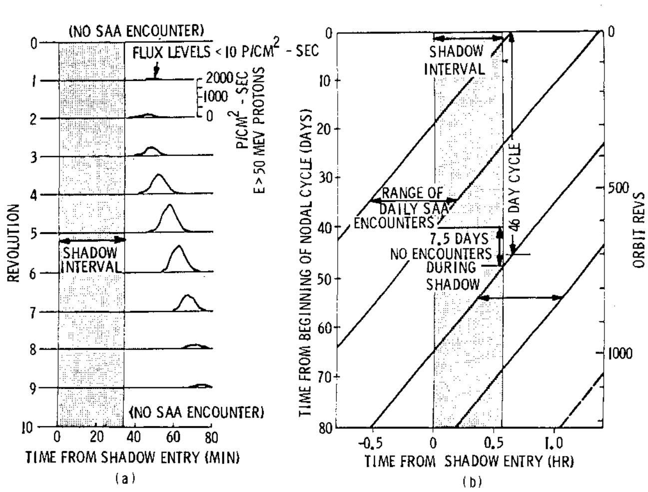

Fig. 17 Cyclic occurrence of SAA encounters relative to ST shadow periods.

As the sun moves along the ecliptic during the year (from right to left in Fig. 15), the S_{10} isophotes follow, defining a seasonal variation of zodiacal brightness at any location in space. Certain types of science observations, for example, observations of faint sources or sensitive photometric experiments, may be limited to periods when the zodiacal light radiance is below a given level.

Radiation Constraints on Viewing

During its orbital lifetime the ST will be exposed to ionizing radiation in the form of high-energy charged particles (e.g., electrons, protons, and heavier nuclei) and electromagnetic radiation (gamma rays, x rays, and ultraviolet light). While geomagnetic shielding at the latitude/altitude range of operation effectively protects against most galactic and solar radiation, particles trapped in the lower Van Allen belt (primarily protons) which strike the light-sensitive detectors of some science instruments will generate photoelectrons and thus false signal levels during an observation. Because of their nature as photon-counting devices, the two cameras onboard the ST will probably not be operated when the vehicle passes through the so-called "South Atlantic Anomaly" (SAA) where the Van Allen belt dips anomalously low. Likewise, induced noise in the fine guidance sensors may prevent holding guide stars through this radiation zone unless they are brighter than a magnitude corresponding to some suitable signal level. On the other hand, operation of the two ST spectrographs and the photometer may be possible in the

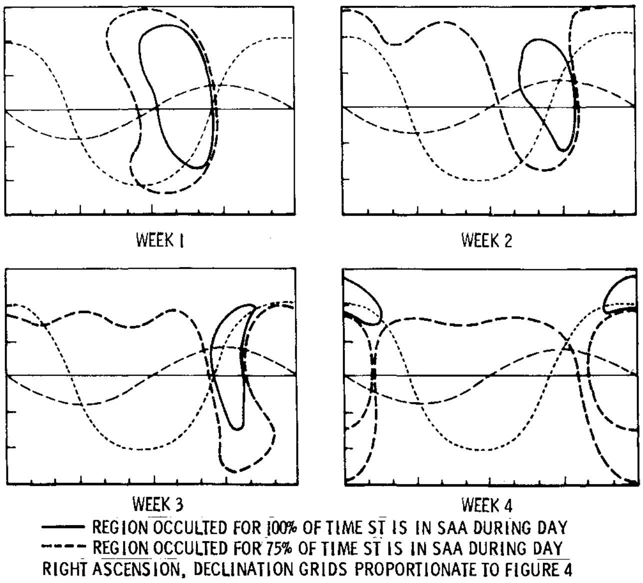

Fig. 18 Evolution of "radiation-free" target regions over four weeks (approximate contours).

SAA, provided the guide stars are held or the observations can be performed while guiding on the vehicle's rate gyro sensors.

As illustrated in Fig. 16, for a 500 km orbit altitude the ST will traverse some portion of the SAA when the longitude of its ascending node is between about 25° W and 175° E.[5] Encounters will regularly occur over eight or nine successive orbit revolutions, with passage times through the Anomaly lasting up to 25 min. Following each series of encounters there is a period of six or seven revolutions (10-12 h) during which no passages occur.

As observations of faint targets will tend to be shadow centered, and many will also be very sensitive to noise caused by external radiation, an important relationship is that between SAA passages and the shadow portion of the ST orbit. While the direction of the Earth's shadow moves very slowly with respect to the celestial sphere, the SAA rotates with the Earth so that successive encounters shift in position relative to ST shadow passages. Figure 17a shows a case where successive SAA encounters all lie in sunlight but, depending on the specific time examined, they may all lie in shadow or in some combination of sunlight and shadow. The time period during which SAA encounters occur during the shadow undergoes a cyclic change as shown in Fig. 17b. The period of this cycling for a 500 km orbit is approximately 46 days, corresponding to the nodal regression period of the orbit adjusted for the motion of the sun-shadow line. During each cycle there is a 7.5 day interval over which no SAA encounters occur within the shadow.

As in the case of shadow viewing discussed earlier, there are regions of the sky which are visible for 100% of the time the ST is passing through the SAA in a series of encounters; such regions would be logically avoided in radiation-sensitive observation scheduling for the time period involved. By the same token, regions of the sky whose occultation periods coincide with SAA passages are favorable for such observing during the eight or nine orbital revolutions which contain encounters. Figure 18 illustrates the evolution of approximate contours of relatively "radiation-free" target regions over a period of a few weeks.

Constraints on Special Science Operations

Special types of Space Telescope operations outside the realm of direct day-to-day scheduling generally have special requirements and constraints associated with them. Many of these physical or operational constraints manifest themselves as constraints on viewing directions or viewing times.

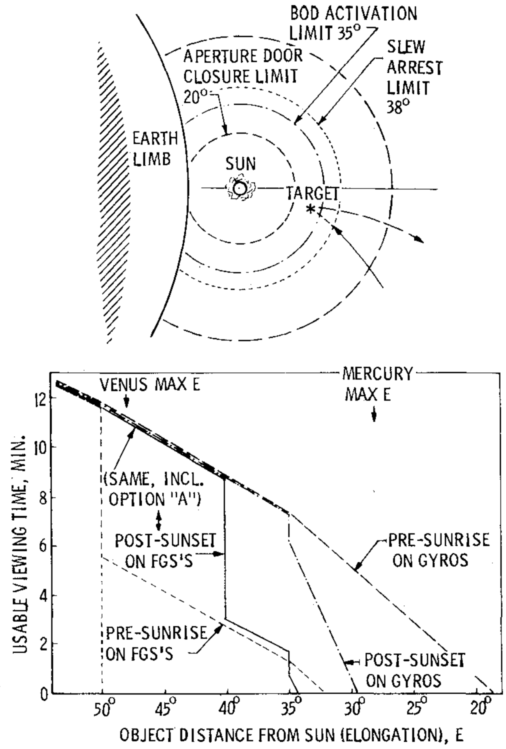

Fig. 19 Characteristics of ST observations close to the sun.

Operation Near the Sun

Occasionally, ST observations may be requested of the two interior planets, minor planets with perihelia inside the Earth's orbit, comets approaching or receding from the sun, or even exterior planets or extrasolar system objects seen within the 50 deg solar stray light reference limit. Although Venus, for example, with a maximum elongation of 48 deg is always inside the 50 deg zone, it spends 119 days of the year farther than 35 deg from the sun. As indicated earlier, some less sensitive observations closer than 50 deg to the sun can probably be scheduled in full sunlight if bright enough guide stars are available or if exposures on rate gyro sensors are adequate. One limitation on such sunlight operation is the fact that for the protection of Space Telescope optics an onboard bright object detector is designed to initiate closure of the spacecraft's aperture door when the view axis approaches 35 deg from the sun. At 38 deg from the sun there is only a very small probability of initiating door closure; beyond 38.4 deg there is essentially no possibility of this because of the physical design of the bright object detector.

While activation of aperture door closure mechanisms based on the detector signal could be inhibited, it may be preferable to avoid the high stray light levels altogether by using the Earth limb as an "occulting disk," i.e., by utilizing observation periods just after orbital sunset or just before orbital sunrise. Figure 19 shows typical fine guidance sensor-tracked or gyro-tracked viewing times which may be available as a function of the distance of a moving object from the sun. It is seen that a short observation on gyros is feasible as close as 18 deg to the sun in the presunrise case, while somewhat more than 4 min are available for observing Mercury at its maximum elongation angle of 28 deg.

Real-Time-Supported Operations

Certain types of Space Telescope science operations will require virtually real-time interaction with the observer or technical support personnel on the ground for varying periods of time—e.g., for acquiring a nebulous target or one in a crowded field or for monitoring science data from an active or unfamiliar object with the intention of modifying the filters to be used, exposure times, or other scientific instrument

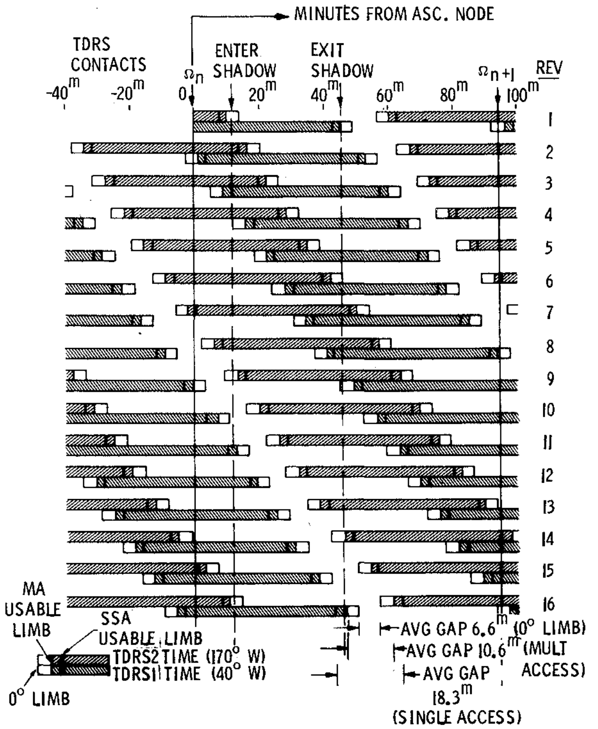

Fig. 20 Variation of TDRS contact times for ST over one day.

parameters. While target viewing time is not directly affected by the need for such operations, the times during the day when the target can be efficiently scheduled for them are affected. ST communications with science and engineering control centers will be exclusively via two synchronous near-equatorial Tracking and Data Relay Satellites (TDRSs), using either a low-data-rate multiple-access mode which can service up to 20 return link users at a time or a higher rate single-access mode which can only support one user at a time. Multiple-access science and engineering telemetry will probably be available continuously whenever a TDRS is in view of the ST, whereas single-access service may be limited to less than 20 min per orbit on the average.

The primary predictable impact of TDRS support on advance scheduling arises because of the TDRS "gap" (or "zone of exclusion") encountered approximately once per ST orbit, a time period during which neither relay satellite is visible (or usable). For equatorial relays separated by 130 deg in longitude the visibility gap averages 6.6 min for the ST orbit described above; however, characteristics of the spacecraft high-gain antennas and international radio restrictions increase the effective downlink transmission gap to 10.6 min for multiple-access data and 18.3 min for single-access data. As shown in Fig. 20, because of the relative orbital motion of the TDRSs with respect to ST the transmission gap is encountered a few minutes later on each successive orbit, causing it for example to "course through" the shadow interval over a day's time. Hence, a shadow-centered target which required rather intensive real-time monitoring over several successive revolutions would have to be scheduled outside of these gap-overlap regions.

Other "predictable" communications-related constraints such as TDRS power restrictions or solar or ground-based-radar interference have similar if somewhat diminished impacts on advance scheduling. In a different class altogether are TDRS scheduling considerations which are basically unpredictable far in advance: for example, failure to obtain a requested communications link because of scheduling conflicts with other users, loss of a scheduled link contact because of a late, high-priority request, or spacecraft inability to acquire a scheduled link for whatever reason. While advance planning can lessen the impact of such occurrences by allowing for delays in crucial contacts, in extreme cases it may be necessary to rely on onboard default operations and to follow pre-established contingency procedures to salvage parts of the affected science program on a short-term basis.

Other ST Operational Constraints

Many other spacecraft hardware subsystems and operational functions exert an indirect influence on target observation scheduling. Frequently a maneuver to a new target or the beginning of guide star acquisition on arrival at a new target may have to be delayed until one or more fixed-head star tracker fields of view become available for a spacecraft attitude update. Occasionally TDRS unavailability will cause onboard data storage capability to be exceeded, so that further observations might have to be suspended until the science tape recorder could be read out. Observations at certain spacecraft roll orientations may be restricted to specific times of the year, to shadow periods, or to small roll angles because of the need to maintain thermal stability and the need for the spacecraft's solar arrays to recharge the onboard batteries. Operations in or near the orbital continuous-viewing zones for extended periods of time may tax certain subsystem component capabilities for thermal dissipation.

Conclusions

The Space Telescope mission planning facility will be required to provide the capability to factor a wide variety of environmental and spacecraft constraint considerations into its day-to-day scheduling functions. Operational timelines incorporating these constraints will be developed to monitor their impact on the performance of the science mission. By noting these interactions sufficiently in advance of the actual generation of onboard command loads, adroit scheduling can usually negate or diminish their impact on operations.

Acknowledgments

This work was supported by NASA Marshall Space Flight Center under Contract NAS8-32697.

References

[1] Bahcall, J.N. and O'Dell, C.R., "The Space Telescope Observatory," *Scientific Research with the Space Telescope, Proceedings of IAU Colloquium No. 54*, U.S. Government Printing Office, Washington, D.C., 1979, p. 5.

[2] Sherrill, T.J. and Hutchinson, P.I., "Space Telescope Design Reference Mission," ST Support Systems Module Data Requirement SE-01, Lockheed Missiles and Space Co., Sunnyvale, Calif., LMSC/D613561A, July 16, 1979.

[3] McWhorter, L.V., 'Pseudo-Stray Light Isochronal Contour (PSLIC) Program" Northrop Services, Inc., Huntsville, Ala., TN-240-1292, June 1974.

[4] Dumont, R., "Photometry of Zodiacal Light and Atmospheric Continuum," *The Zodiacal Light and the Interplanetary Medium*, NASA SP-150, Jan-Feb. 1967, pp. 63-69.

[5] Lavine, J.P. and Vette, J.I., "Models of the Trapped Radiation Environment," NASA SP-3024, 1966.